

ESTIMATION OF CRITICAL FRONTAL PROCESS ZONE SIZE IN CERAMICS

Hideo Awaji, Chun-Hong Chen, Nobuyuki Kishi, and Seong-Min Choi
 Dept. Materials Engng., Nagoya Institute of Technology
 Gokiso-cho, Showa-ku, Nagoya, 466-8555 Japan
 awaji.hideo@nitech.ac.jp

Abstract

A macroscopically defined critical frontal process zone (CFPZ) size ahead of a crack tip is estimated for alumina ceramics, alumina-based nanocomposites, and porous alumina ceramics. A three-point flexure test is carried out systematically on alumina using flexural specimens with various depths of a sharp V-shaped notch. The relation between the flexural strength and the local fracture stress is clarified based on the Griffith criterion and the local fracture criterion, and the formula for the relation between the strength and the notch depth is successfully established.

Introduction

The aim of this paper is to propose an indirect technique for estimating a macroscopically defined critical frontal process zone (CFPZ) size using the SEVNB (single-edge V-notched beam) method [1,2] to clarify the toughening mechanism of ceramics. The relation between strength, fracture toughness, and CFPZ size of alumina ceramics, alumina-based nanocomposites, and porous materials is estimated based on the Griffith criterion [3] and the local fracture criterion [4] using the exact stress distribution around a crack tip.

Theory

Griffith-Irwin criterion

The Griffith energy equilibrium states that a necessary condition for crack extension is that the energy needed to create a new fracture surface be supplied the released strain energy [1]. Accordingly, when the energy release rate, $G = dU/da$, equals the fracture energy rate required for crack growth, $R = dW/da$, crack growth can occur, where dU is the released strain energy during infinitesimal crack growth and dW is the increased fracture energy during the growth. For mode I loading, the energy equilibrium of crack growth in an infinite plate is expressed under the condition of small-scale yielding using the Irwin's notation as [5]

$$\frac{K_{IC}^2}{E'} = 2\gamma_I \quad , \quad (1)$$

where γ_I represents the mode I fracture energy per unit crack-surface area when the crack extends in its own direction, namely, the direction of the maximum energy release rate, K_{IC} is the fracture toughness, $E' = E$ for plane stress condition and $E' = E/(1 - \nu^2)$ for plane strain condition, E is Young's modulus and ν is Poisson's ratio. This equation is called the Griffith-Irwin Criterion. The superior feature of the Griffith concept is that the equation for the energy equilibrium is composed of two discrete parts. The first part is the energy-release rate expressed on the left side of Eq. (1). The energy-release rate is independent on the nonlinear

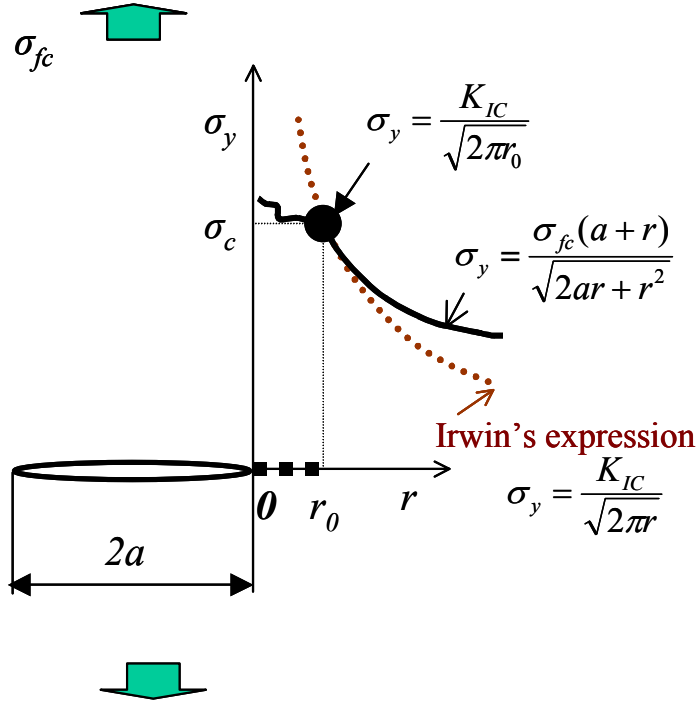


FIGURE 1. Stress distributions around a crack tip.

stress state in the frontal process zone (FPZ) ahead of a crack tip. In other words, the energy release rate is precisely determined by the stress intensity factor that depends on only the conditions of the outer boundary such as the applied remote stress and the specimen geometry, as long as the condition of small-scale yielding is applicable. The second part is the fracture energy rate expressed on the right side of Eq. (1), which is directly related to the microstructure in the FPZ and the size of the FPZ, representing the crack resistance of the material that must be overcome for crack growth to occur, and should be a material constant.

Local fracture criterion

The local fracture criterion [4] states that a crack will propagate when the stress at the characteristic distance from the crack tip reaches the local fracture stress, σ_c , shown in Fig. 1.

Figure 1 shows the stress distributions around a crack tip, where the solid curve indicates exact stress distribution under a critical stress state ($K_I = K_{IC}$) and the dotted curve is its stress intensity approximation called Irwin's expression. It should be noted that if the characteristic distance from the crack tip is equal to the CFPZ size, the Griffith-Irwin criterion and the local fracture criterion become identical, which gives the following relation between the fracture toughness and the local fracture stress, under the small-scale yielding condition

$$\sigma_c = \frac{K_{IC}}{\sqrt{2\pi r_0}} \quad (2)$$

where r_0 represents the CFPZ size. The important point is that the local fracture criterion satisfies the Griffith energy equilibrium when the characteristic distance is equal to the CFPZ size. From Eq. (2), the CFPZ size is expressed as,

$$r_0 = \frac{1}{2\pi} \left(\frac{K_{IC}}{\sigma_c} \right)^2 . \quad (3)$$

Therefore, if we know the σ_c value, we can estimate the CFPZ size.

When linear fracture mechanics is not applicable, namely in the case of short crack length compared with the r_0 value, the difference between the exact stress and the Irwin's expression becomes large at the location of r_0 , as shown in Fig. 1. Then, we have to use the exact stress formula to assess the local fracture stress. The exact stress formula on the r -axis in an infinite plate with a crack of length, $2a$, under a remote stress, σ_f , is expressed as [7]

$$\sigma_y = \frac{\sigma_f(a+r)}{\sqrt{2ar+r^2}} = \sigma_f F_c(r) . \quad (4)$$

The following relation is then derived based on the local fracture criterion

$$\sigma_c = \sigma_{fc} F_c(r_0) , \quad (5)$$

where σ_{fc} is the critical remote stress (strength) of the center-cracked infinite plate. From Eq. (5), the following equation is derived:

$$\sigma_{fc} = \frac{\sigma_c}{F_c(r_0)} . \quad (6)$$

This equation indicates the relation between the strength of the center-cracked infinite plate and the local fracture stress.

Experimental Procedure and Results

Flexure test for V-notched specimen

We used a three-point flexure test called the SEVNB method [1,2] to estimate the local fracture stress and the CFPZ size. The material is polycrystalline alumina (99.5% pure with MgO as minor dopant, Japan Fine Ceramics Center), alumina-based nanocomposites ($\text{Al}_2\text{O}_3/5\text{wt}\%\text{Ni}$, $\text{Al}_2\text{O}_3/3\text{vol}\%\text{SiC}$) [8,9], and porous alumina [10]. The sharp V-shaped notch was machined carefully into the flexural specimens using a V-shaped diamond wheel. The root radius of the machined notch was less than 20 μm . The specimens were $3 \times 4 \times 40 \text{ mm}^3$ in size. Three-point flexure tests were carried out on the specimens without the machined notch or with notches of various depths.

Flexural strength vs. crack length

Figure 2 shows the experimental results of the relation between the flexural strength and the equivalent crack length for alumina. The equivalent crack length in an infinite plate is used to remove the influence of the shape factor, Y , on the fracture strength of the notched specimen [11,12]. The stress intensity factor of the edge-cracked flexural specimen is expressed as

$$K_I = Y\sigma\sqrt{a} . \quad (7)$$

The equivalent crack length is then calculated as

$$a_e = \frac{Y^2}{\pi} a . \quad (8)$$

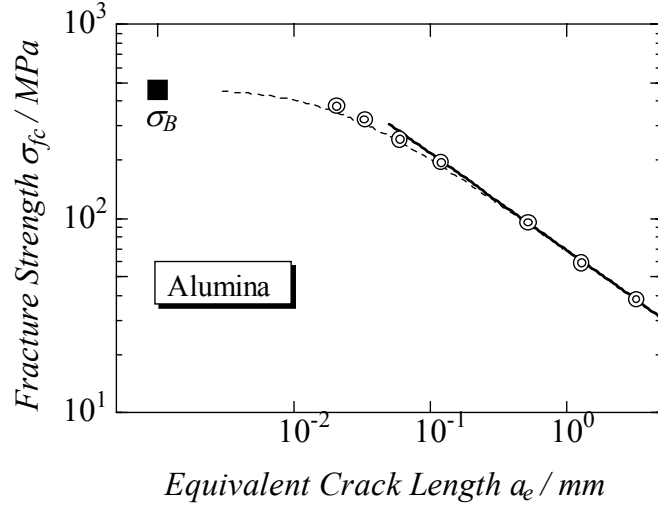


FIGURE 2. Experimental results of the flexural strength vs. equivalent crack length.

In Fig. 2, the solid square (■) indicates the flexural strength of the un-notched specimens, where the mean strength was 462 ± 18.0 MPa with the shape factor of Weibull distribution, $m = 28$, and the scale factor, $\beta = 471$ MPa. The double-circles (⊙) indicate the strength of the notched specimens and the nominal notch length are 0.01, 0.02, 0.05, 0.1, 0.5, 1.0, and 1.5 mm. The fracture toughness estimated from the data on the $-1/2$ gradient line is $3.72 \text{ MPam}^{1/2}$ using a least square approximation.

Discussion

Local fracture stress

The maximum stress on the tensile surface of a rectangular shaped three-point flexural specimen is expressed as

$$\sigma_f = \frac{3PS}{2W^2H} \quad (9)$$

Considering a flexural specimen with an edge crack, as shown in Fig. 3, the imagined remote flexural stress at the distance from the notch tip, r , is expressed as

$$\sigma(r) = \sigma_f \frac{W - a - 2r}{W - a} \quad (10)$$

The exact stress at r around an edge crack is then expressed as

$$\sigma_y(r) = \sigma(r)F_c(r) \quad (11)$$

The local fracture stress at r_0 can be derived as

$$\sigma_c = \sigma_{fc} \frac{W - a - 2r_0}{W - a} F_c(r_0) \quad (12)$$

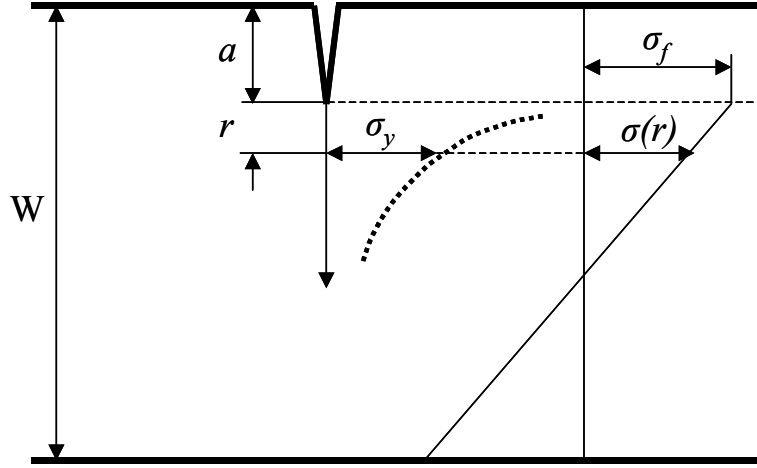


FIGURE 3. Exact stress distribution around an edge crack in a flexural specimen.

and the strength of the specimen with an artificial crack is expressed as

$$\sigma_{fc} = \sigma_c \frac{W - a}{W - a - 2r_0} \frac{1}{F_c(r_0)} \quad (13)$$

Because of the relation $W \gg 2r_0$, the following relation is derived from Eq. (13)

$$\lim_{a \rightarrow 0} \sigma_{fc} \rightarrow \sigma_c \quad (14)$$

This equation indicates that the local fracture stress, σ_c , is the flexural strength when the artificial crack length reduces to zero. However, the σ_c is not equal to the σ_B , where the σ_B is the flexural strength of the specimen with no artificial crack, because the σ_B depends on the maximum defect size intrinsically existing in the specimen. The size effect on the strength of the flexural specimen and the CFPZ size is able to explain the difference between the strengths σ_B and σ_c .

The effective volume of the three-point JIS type specimen is expressed as [13]

$$V_{e3} = \frac{V}{2(m+1)^2} \quad (15)$$

where $V (=WBS)$, W : width of the specimen, B : thickness of the specimen, S : span length) is the effective volume of the flexural specimen. The V is calculated to be $3 \times 30 \text{ mm}^2$ for unit thickness ($B = 1$).

The CFPZ size of alumina is $6.9 \text{ }\mu\text{m}$, details of which will be explained later. The FPZ of ceramics is considered an area enclosed by a contour of the principal stress. Thus the effective volume of the CFPZ, V_{FPZ} , is roughly estimated to be $6.9 \times (2 \times 6.9) \times 10^{-6} \text{ mm}^2$ for unit thickness. In addition, the FPZ is considered to be an equi-biaxial stress state because the FPZ is composed of nano-cracks. Therefore, the ratio of the strength between the specimen under a uniform uni-axial stress state and the specimen under an equi-biaxial stress state can be expressed as [13]

$$\frac{S_2}{S_1} = \left(\frac{1}{1 + \mu^m} \right)^{1/m} \quad (16)$$

where, S_1 represents the strength of the specimen under a uni-axial stress, S_2 is the strength under an equi-biaxial stress, μ is the stress ratio of the biaxial stresses. In the case of equiaxial stress state, $\mu = 1$.

The ratio of the local fracture stress and the three-point flexural strength is then calculated from the following equation:

$$\frac{\sigma_c}{\sigma_B} = \left\{ \frac{V_{e3}}{V_{FPZ}} \right\}^{1/m} \cdot \frac{S_2}{S_1} \quad (17)$$

Using $m = 28$ and $\sigma_B = 462$ MPa, we obtain $\sigma_c = 565$ MPa.

Figure 4 shows the relation between the experimentally obtained flexural strength of un-notched specimens (■) and the local fracture stress (◆), where the dot-dashed curve indicates the calculated value of σ_{fc} from Eq. (6), assuming the CFPZ size to be $6.9 \mu\text{m}$. The dotted curve is obtained using the σ_B instead of σ_c in Eq. (6). The experimentally obtained flexural strengths of the notched specimens indicated by the double-circles lie on the dot-dashed curve rather than on the dotted curve.

Critical frontal process zone size

The local fracture stress can be estimated for each notched specimen. The results are shown in Fig. 5. It should be noted that every local fracture stress of the notched specimen has the almost same value, where the CFPZ size is assumed $6.9 \mu\text{m}$. This CFPZ size is not the actual FPZ size. The CFPZ size depends on the microstructure ahead of the crack tip, and the shape of the leading edge of the crack depends on the microstructure, such as grain size, grain boundary, defects, and dispersed particles. Then the CFPZ size varies place to place. Therefore, the CFPZ size estimated from Eq. (3) should be considered a macroscopically defined value, because the CFPZ size is calculated from the macroscopically defined values of the fracture toughness and the local fracture stress. The actual CFPZ size observed by a microscopy is quite small [14].

Fracture toughness vs. critical frontal process zone size

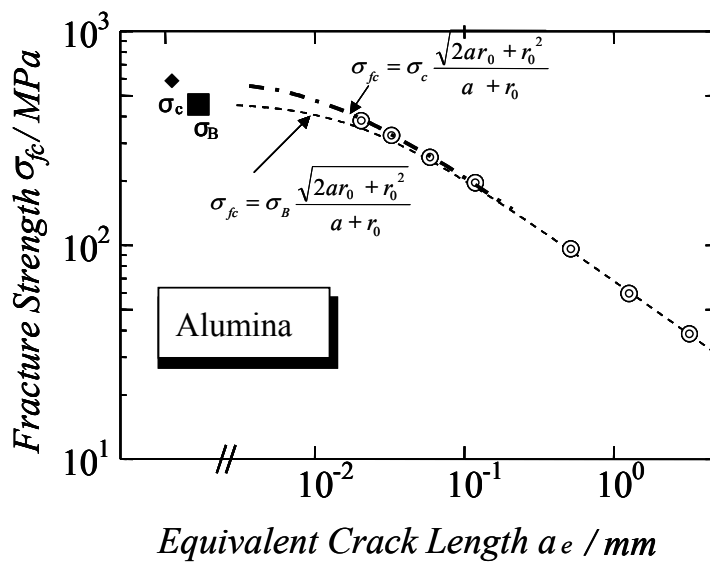


FIGURE 4. Experimentally obtained flexural strength of notched specimens, flexural strength of un-notched specimen, and local fracture stress.

From Eq. (2), the following relation between the strength and the fracture toughness is derived

$$K_{IC} = \sigma_c \sqrt{2\pi r_0} \approx \sigma_B \cdot r_0^{1/2} \tag{18}$$

Figure 6 shows the relation between the fracture toughness and $\sigma_B \cdot r_0^{1/2}$ for several ceramics. The experimental data for these materials are summarized in Table 1. Figure 6 implies that improvement of the fracture toughness requires greater values of both the strength and the CFPZ size.

Conclusions

We presented the technique for estimating the critical frontal process zone (CFPZ) size for ceramics, using the single-edge V-notched beam (SEVNB) method. A three-point flexure test was conducted on alumina specimen with several depths of V-notch. The local fracture stress was analysed based on the Griffith energy criterion and the local fracture criterion. The macroscopically defined CFPZ size was estimated to be 6.9 μm for alumina. The relation

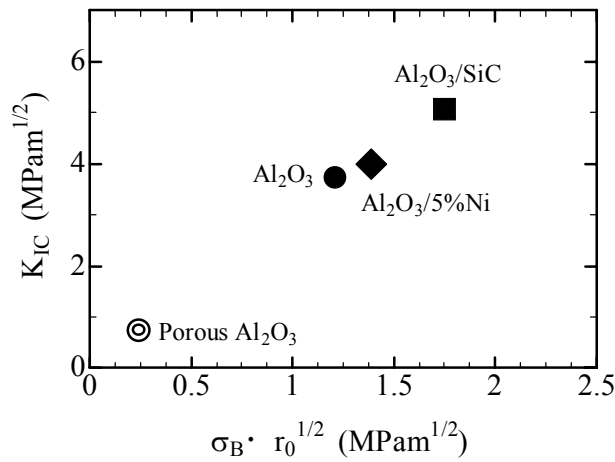


FIGURE 6. Relation between the fracture toughness and $\sigma_B \cdot r_0^{1/2}$ of alumina-based materials.

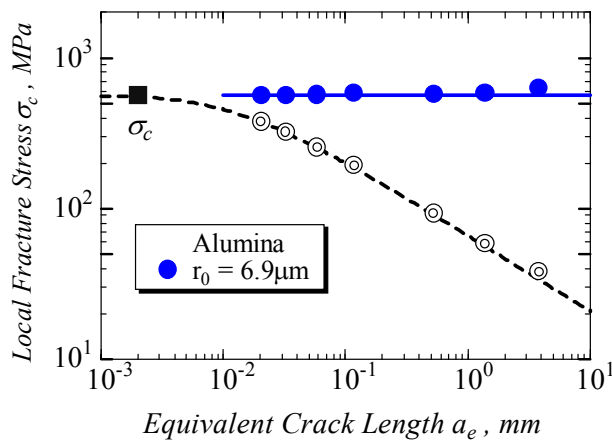


FIGURE 5. Local fracture stresses at the CFPZ size of each notch depth.

Table 1. Summary of the data.

Specimen	Strength σ_B (MPa)	Fracture toughness K_{IC} (MPa·m ^{1/2})	Critical FPZ size r_0 (μ m)	$\sigma_B \cdot r_0^{1/2}$ (MPa·m ^{1/2})
Al ₂ O ₃	462	3.72	6.9	1.21
Porous Al ₂ O ₃	38.4	0.75	39.7	0.24
Al ₂ O ₃ / 5wt%Ni	462	4.00	9.0	1.39
Al ₂ O ₃ / 3vol%SiC	760	5.06	5.3	1.75

between the strength and the notch depth was successfully established using the exact stress distribution around the crack tip. The relation among the fracture toughness, the strength, and the CFPZ size was derived as

$$K_{IC} \propto \sigma_B \cdot r_0^{1/2} .$$

This equation suggests that both the strength and the CFPZ size must be increased to improve the fracture toughness of ceramics. Some experimental results for ceramics were demonstrated to show this relation.

References

1. Awaji, H. and Sakaida, Y., *J. Am. Ceram. Soc.*, vol. **73**, 3522-23, 1990.
2. Awaji, H., Watanabe, T., Yamada, T., Sakaida, Y., Tamiya, H., Nakagawa, H., *Trans. Japan Soc. Mech. Eng.*, vol. **56**, 1148-53, 1990 (in Japanese)
3. Griffith, A.A., *Trans. Roy. Soc. London*, **A221**, 163-197, 1920.
4. Strandberg, M., *Engng. Fract. Mech.*, vol. **69**, 403-415, 2002.
5. Broek, D., *Elementary Engineering Fracture Mechanics*, 4th ed., Kluwer Academic Pub., 1986.
6. Lawn, B., *Fracture of Brittle Solids*, 2nd ed., Cambridge Univ. Press, 1993.
7. Awaji, H., Watanabe, T., and Sakaida, Y., *Ceramics Int.*, vol. **18**, 11-17, 1992.
8. Choi, S-M., Honda, S., Nishikawa, T., Awaji, H., Sekino, T., and Niihara, K., *J. Soc. Mater. Sci. Japan*, vol. **52**, 1374-1378, 2003 (in Japanese).
9. Choi, S-M., *Structural Integrity and Fracture*, Eds. Dyskin, A. V., Hu, X., and Sahouryeh, E., Swets & Zeitlinger, Lisse, 2002.
10. Kishi, N. Master-degree thesis, 2003, Nagoya Institute of Technology (in Japanese).
11. Usami, S., Kimoto, H., Takahashi, I., and Sida, S., *Eng. Fract. Mech.*, vol. **23**, 745-761, 1986.
12. Kimoto, H., Usami, S., and Miyata, H., *Trans., Japan Soc., Mech. Engineers*, vol. **51**, 2482-2488, 1985 (in Japanese).
13. Awaji, H., *Strength of Ceramic Materials*, Corona Pub., Tokyo, 2001 (in Japanese).
14. Ikuhara, Y., Suzuki, T., and Kubo, Y., *Philosophical Magazine Lett.*, vol. **66**, 323-327, 1992.